ARTICLES

Propagation of a topological transition: The Rayleigh instability

Thomas R. Powers
Department of Physics, University of Arizona, Tucson, Arizona 85721

Dengfu Zhang[a)]
Division of Engineering and Applied Sciences, Harvard University, Cambridge, Massachusetts 02138

Raymond E. Goldstein
Department of Physics and Program in Applied Mathematics, University of Arizona, Tucson, Arizona 85721

Howard A. Stone
Division of Engineering and Applied Sciences, Harvard University, Cambridge, Massachusetts 02138

(Received 21 August 1997; accepted 1 December 1997)

The Rayleigh capillary instability of a cylindrical interface between two immiscible fluids is one of the most fundamental in fluid dynamics. As Plateau observed from energetic considerations and Rayleigh clarified through hydrodynamics, such an interface is linearly unstable to fission due to surface tension. In traditional descriptions of this instability it occurs everywhere along the cylinder at once, triggered by infinitesimal perturbations. Here we explore in detail a recently conjectured alternate scenario for this instability: front propagation. Using boundary integral techniques for Stokes flow, we provide numerical evidence that the *viscous* Rayleigh instability can indeed spread behind a front moving at constant velocity, in some cases leading to a periodic sequence of pinching events. These basic results are in quantitative agreement with the marginal stability criterion, yet there are important qualitative differences associated with the discontinuous nature of droplet fission. A number of experiments immediately suggest themselves in light of these results. © *1998 American Institute of Physics.* [S1070-6631(98)00504-2]

I. INTRODUCTION

Recently, Bar-Ziv and Moses discovered the ''pearling instability'' of lipid bilayer membrane tubes, in which the application of laser tweezers to the membrane induces a periodic modulation in the radius.[1] Theoretical explanations[2] for this behavior invoke a tension created in the membrane by the laser tweezers. Were this an interface between two immiscible fluids, such tension would induce capillary breakup of the cylinder into droplets via the Rayleigh instability.[3] In the pearling phenomenon however, breakup is prevented by the membrane bending elasticity. A more striking difference is that the pearling instability propagates—the modulated state is observed to invade the uniform cylindrical region at a constant velocity. This propagation is totally unlike traditional descriptions of the Rayleigh instability,[4] in which each sinusoidal perturbation grows uniformly along the length of the tube. Note that this propagation cannot be described by a superposition of traveling waves moving at the front velocity, since the regions a few wavelengths ahead and behind the moving front are stationary.

In a previous publication,[5] we conjectured that the viscous Rayleigh instability can propagate as well. Propagating fronts in which a new stable state invades an unstable region are a common feature of overdamped systems,[6] arising in such diverse situations as reaction-diffusion systems, dendritic growth, and, more recently, type-I superconductors.[7] These previously well-studied examples all display a *continuous* evolution, in contrast to the discontinuous evolution associated with drop fission. Below we show by numerical methods that despite this fundamental difference, the Rayleigh instability of a cylindrical interface can indeed propagate. Furthermore, the coarse features of this behavior can be described by the *marginal stability criterion* (MSC), an analytical method which has found wide applicability in the simpler situations mentioned above.[8]

The discontinuous evolution associated with rupture of the thread can have significant implications for the possible existence of a propagating front. As a droplet pinches off from the main body, the two tips of the broken neck recede from the pinching point; if the retracting end overtakes the front, propagation will be spoiled. Experiments on the breakup and relaxation of elongated drops suspended in an outer fluid[9] reveal that this competition depends on the relative viscosity of the two fluids. When the drop viscosity η^- is much smaller than the outer viscosity η^+, the drop breaks before its ends have time to retract; in the other extreme, the ends retract significantly before breaking off (for long enough drops). We shall see below that when the viscosity ratio $\lambda = \eta^-/\eta^+$ is such that retraction is slow on the time scale for breakup, there is a propagating front moving with constant velocity (Fig. 1). No analytical solution is known

[a)]Present address: Adapco, 60 Broadhollow Rd., Melville, NY 11747.

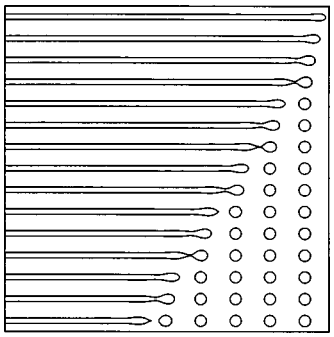

FIG. 1. Sequence of drop shapes for viscosity ratio $\lambda=0.05$ at $t_n=6.67m\eta^+R_0/\gamma$; $n=1,2,3,\ldots,15$ from top to bottom. To illustrate the complete evolution, we have drawn the daughter droplets (but not the satellite droplets). However, the evolution of each connected component was computed independently of the others.

for the complex shape evolution shown in Fig. 1. Indeed, this is the case in most examples of front propagation, where, however, the MSC nearly always provides correct predictions for the front speed. In our studies of drop breakup below we find that the front speed is rather accurately given by the linear MSC, a remarkable result in light of the strongly nonlinear, singular shape evolution behind the front.[10] In addition to the front velocity, we compute the time between primary pinching events in the breakup of the cylinder using the MSC quantities and find good agreement with the numerical calculations.

II. DROP EVOLUTION

We look for the propagation of the Rayleigh instability in a numerical simulation of a long, axisymmetric, approximately cylindrical drop, initially stationary and with hemispherical caps on the ends. The axis of the cylinder defines the x-direction, so that the shape is given by the surface of revolution generated by the radius $R(x)$. We work in the overdamped limit in which the inertial terms of the Navier–Stokes equations may be neglected. Therefore, the outer and inner fluids with velocities $\mathbf{u}^{\pm}$ and pressures $p^{\pm}$ are described by the Stokes equations and the constraint of incompressibility

$$\eta^{\pm}\nabla^2\mathbf{u}^{\pm}=\boldsymbol{\nabla}p^{\pm},\quad \boldsymbol{\nabla}\cdot\mathbf{u}^{\pm}=0. \tag{1}$$

Propagation in the inertial regime is complicated by the presence of dispersive capillary waves, and we leave this case and the case of net flow (like a jet) for future work. The boundary conditions at the interface S are continuity of fluid velocity $\mathbf{u}^+|_S=\mathbf{u}^-|_S$, continuity of tangential stress, and the jump in normal stress:

$$n_i(\sigma_{ij}^+-\sigma_{ij}^-)|_S=-2\gamma Hn_j, \tag{2}$$

where $\mathbf{n}$ is the outward surface normal, H is the mean curvature, γ is the (constant) interfacial tension, and the stress tensors are $\sigma_{ij}^{\pm}=\eta^{\pm}(\nabla_i u_j^{\pm}+\nabla_j u_i^{\pm})-p^{\pm}\delta_{ij}$. For an axisymmetric shape with radius $R(x)$, and with $R_x\equiv\partial R/\partial x$, the mean curvature is $H=(R_{xx}/2)(1+R_x^2)^{-3/2}-(2R)^{-1}(1+R_x^2)^{-1/2}$. The only important material parameters are therefore the surface tension γ and the viscosities η^+ and η^-.

Note that (2) gives rise to the *absolute* (rather than convective) instability of a stationary cylindrical interface. When the fluid velocity is zero, the pressure jump across the interface is $\Delta p=2\gamma H$. Consider an axisymmetric perturbation in which the radius is slightly pinched to form a neck. If the disturbance is of sufficiently long wavelength, the magnitude of the curvature is increased, thus raising the pressure in the neck. Fluid is therefore forced out of the pinched region, leading to growth of the perturbation.

The challenging numerical task of solving the three-dimensional Stokes equations is greatly simplified by the boundary integral technique, in which (1) and (2) are recast as an integral equation for quantities on the interface.[11] This approach removes one spatial dimension from the problem, leading to

$$\frac{(1+\lambda)}{2}u_j(\mathbf{y})=\frac{\gamma}{4\pi\eta^+}\int_S H(\mathbf{x})n_i(\mathbf{x})J_{ij}(\mathbf{x},\mathbf{y})\mathrm{d}S(\mathbf{x})+\frac{(1-\lambda)}{4\pi}\mathscr{P}.\mathscr{V}.\int_S u_i(\mathbf{x})n_k(\mathbf{x})K_{ijk}(\mathbf{x},\mathbf{y})\mathrm{d}S(\mathbf{x}), \tag{3}$$

where $\mathbf{y}$ is a point on the interface S, $\mathbf{u}(\mathbf{y})$ is the velocity of the interface at $\mathbf{y}$, $\mathscr{P}.\mathscr{V}.$ denotes the principal value, and the kernels J_{ij} and K_{ijk} are Green's functions.[12]

Axisymmetry reduces our problem to an integral equation with one space and one time dimension. This equation is solved numerically by standard adaptive-grid techniques[13] to yield the interfacial velocities, and so the drop shape, as a function of time. This procedure can describe the continuous motion of the interface only; to describe the breakup of the interface we simply demand that pinching occurs whenever the radius $R(x)\leqslant 0.005R_0$, where R_0 is the initial cylinder radius. Although somewhat arbitrary, we expect this choice for the cutoff leads to little error in the gross evolution since further decreases in the neck radius occur rapidly owing to the large velocity and curvature gradients near the pinch point. Furthermore, the size of the region in which these quantities grow large is small.[14] In any case, these same factors make it difficult to do numerical calculations when the neck approaches rupture. Once a droplet has pinched off, we neglect it in further calculations, since experience has shown the the evolution of the droplet that pinches off has little effect on the evolution of the main drop.[15]

Our findings for the shape evolution are in qualitative accord with previous investigations.[9] At higher values of λ, i.e. around $\lambda=10$, the evolution is dominated by retraction. As an example, Fig. 2 shows that the $\lambda=10$ drop simply retracts and shows no sign of developing a neck in the time it takes the $\lambda=0.1$ drop to break a few times. Figure 3 shows a magnified view of the evolution of these droplets. Note that at a given time the radius $R(x)$ of the $\lambda=10$ drop grows monotonically in x to its maximum value, but the radius for $\lambda=0.1$ is modulated; these undulations are the seeds of the capillary instability.

When the outer viscosity is not too small, we can estimate the retraction speed by assuming the bulge on the drop

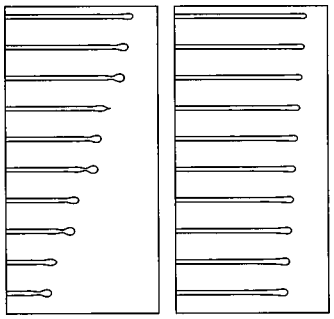

FIG. 2. Numerical results. Propagation of the Rayleigh instability for $\lambda=0.1$ (left). Retraction-dominated dynamics for $\lambda=10$ (right). $t_n=6.67n\eta^+R_0/\gamma$, where $n=1,2,3,\ldots,10$ labels the shapes from the top.

end is spherical and balancing tension with drag.[5] This leads to a velocity that scales like γ/η^+, since the drag on a liquid sphere suspended in another fluid is controlled by the outer viscosity.[16] This estimate only accounts for the dissipation due to the flows in the two fluids induced by pulling a spherical interface through the outer fluid; it disregards the contribution due to shape change, which become comparable when $\lambda\geqslant 1$. Indeed, when there is no outer fluid all the dissipation takes place inside the retracting end. Our estimate is little more than dimensional analysis. Nevertheless, it is borne out by the simulations: if we take the retraction velocity to be the speed of the maximum of $R(x)$ nearest the end of the drop (Fig. 4), we find retraction velocities that range from $0.2\gamma/\eta^+$ at $\lambda=0.005$ to $0.1\gamma/\eta^+$ for $\lambda=10$.

The front region connects the uniform cylinder, which has not yet undergone the Rayleigh instability, to the growing bulge, which eventually pinches off (Fig. 4). We extract the front from the sequence of drop shapes by choosing for each shape a window with one edge such that $R(x)$ is within numerical accuracy of the unperturbed radius R_0, and the other edge with $|R(x)-R_0|/R_0$ reaching a small value a^* (typically 0.1–0.15). The drop radius in this window is fit[17] with an exponential envelope times a sinusoidal function of the form $R(x)=a_1+a_2\exp(-q''_{\rm num}x)\cos(q'_{\rm num}x-a_3)$. We find that the fit parameters a_1, a_2, a_3, $q'_{\rm num}$, $q''_{\rm num}$ do not change with small changes in the choice of fitting window or small changes in the initial shape of the ends of the drop. The front speed is the velocity of the point $x_f(t)$ for which the envelope function $a_2\exp(-q''_{\rm num}x_f(t))=a^*$.

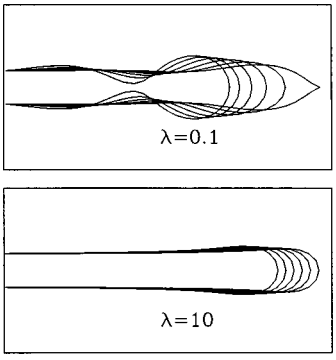

FIG. 3. Enlarged view of the droplet ends of Fig. 2 for $\lambda=0.1$ and $\lambda=10$. $t_n=(37.5+3n)\,\eta^+R_0/\gamma$, where $n=1,2,\ldots,6$ labels the shapes.

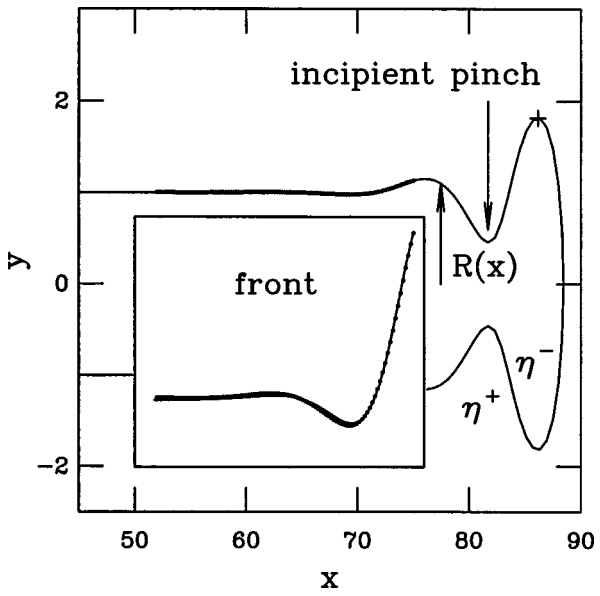

FIG. 4. A snapshot of the end of the main drop for $\lambda=0.05$, in which the aspect ratio has been distorted to show the front more clearly. The center of the drop is at $x=0$. The darkened line is the front region; the inset is a magnified view of this region (solid line) and a fit to the front (dotted line). The retraction speed is taken to be the velocity of the maximum marked with a plus sign.

Turning now to the analysis of the fronts, we find a smoothly moving front for a range of viscosity ratios, from $\lambda=0.005$ to $\lambda=1.0$. For example, the top graph in Fig. 5 shows the front position as a function of time for $\lambda=0.05$. At low values of λ, around $\lambda=0.005$, the ends do not retract much before the drop pinches (Fig. 2). This is the ''end-pinching'' behavior described in Ref. 9: the daughter droplets pinch off one at a time in a periodic fashion at the ends of the main drop.[18] Despite the discrete nature of these events, there is a front moving smoothly at constant velocity.

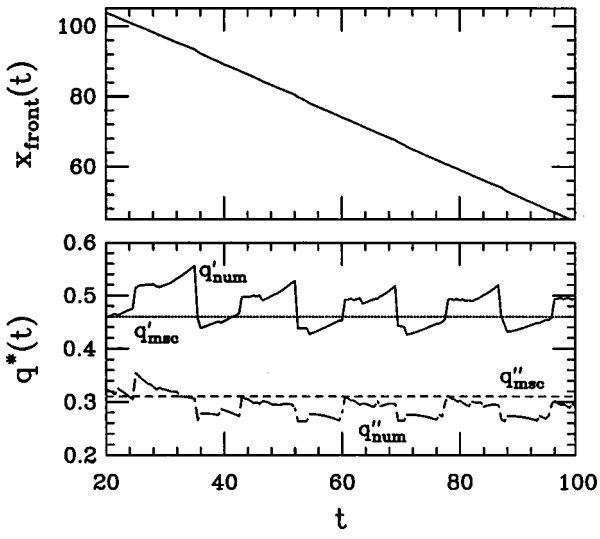

FIG. 5. Top: results of boundary integral calculations and fitting routine for front position vs time. Bottom: comparison of prediction of MSC and results of boundary integral method for the initial front wavenumber q' and front width q''. Both plots are for $\lambda=0.05$. The simulation begins at $t=0$; by $t\gamma/(\eta^+R_0)=20$ transients from the initial shape have died out.

We therefore interpret this end-pinching at low viscosity ratio as a front of the Rayleigh instability.

As λ increases, retraction becomes more apparent in the time it takes the droplets to break off. When λ reaches a value at which the retraction speed becomes comparable to the speed at which the pinches are spreading (around $\lambda=1$), we find that the drop evolution can not be described as a smoothly moving front. The details of this process are complicated. For $\lambda\approx 0.2$, the periodic behavior of the breakup ceases. The droplets that pinch off are not of uniform size and do not pinch off at a constant rate. Nevertheless, we are still able to fit the advancing profile to a front moving smoothly with constant velocity. When $\lambda>1.0$, this smoothly propagating front behavior is lost. Around this value of λ we also observe necks that start to form at one point but then heal, leading to breakup at a different point along the drop. This behavior is reminiscent of that seen in the experiments of Tjahjadi *et al.*, who observed that a drop stretched to a cylindrical shape just beyond the critical aspect ratio for breakup does *not* break.[19] Instead, two necks form and then disappear, and the elongated drop retracts to a sphere without breaking. We can offer no explanation of this behavior, and merely note that when retraction is faster than the pinching process, there is no reason to expect the simple picture of the Rayleigh instability outlined in the last section to apply.

III. FRONT VELOCITY AND MSC

For completeness, we review first the basic facts of the marginal stability criterion. In the leading edge of the front, the amplitude $h(x,t)\equiv R(x,t)-R_0$ is small and can be represented as a linear combination of Fourier modes each having the form $h(x,t)\propto \mathrm{Re}\{\exp(\omega(q)t+iqx)\}$, in which $\omega(q)$, possibly complex, is the linear growth rate, and the real and imaginary parts of the wavevector q describe the periodicity and sharpness of the mode, respectively. The velocity of the exponential envelope of any mode is $v_q=\mathrm{Re}\,\omega/\mathrm{Im}\,q$. The MSC selects a unique mode $q^*=q'_{\mathrm{msc}}+iq''_{\mathrm{msc}}$ (and hence velocity v_{msc}) by the condition that the envelopes of modes nearby in q neither outrun nor fall behind that of q^*. This condition provides two additional relationships between v_{msc} and q^*, leading to the conditions[8,20]

$$v_{\mathrm{msc}}=\frac{\mathrm{Re}\ \omega^*}{\mathrm{Im}\ q^*},\quad \mathrm{Re}\left.\frac{\partial\omega}{\partial q}\right|_{q^*}=0,\quad v_{\mathrm{msc}}=-\,\mathrm{Im}\left.\frac{\partial\omega}{\partial q}\right|_{q^*}. \qquad (4)$$

A rigorous proof of the validity of this approach is known only for the Fisher–Kolmogorov equation,[21] $h_t=h_{xx}+h-h^3$, for which it can be shown that sufficiently localized initial conditions will evolve into a front moving at a unique speed[22] $v=v_{\mathrm{msc}}$. Many partial differential equations have been shown to be correctly described by this principle or its nonlinear variants,[8] even when no analytic front solution is known. There is, however, no general criterion to determine when the MSC is applicable, and thus the question of its validity in this new setting of discontinuous evolution is of interest.

The MSC quantities depend only on the growth rate ω, which is known from Tomotika's generalization[23] of Rayleigh's result to the two-fluid problem. For a cylinder of radius R_0, ω is a function of wave vector q and viscosity ratio λ in the form $\omega(q,\lambda)=(\gamma/R_0\eta^+)\Lambda(q,\lambda)(1-q^2R_0^2)$. The dynamical factor $\Lambda(q,\lambda)$, too lengthy to quote here, accounts for viscous dissipation, and the factor $\gamma(1-q^2R_0^2)$ is associated with the Young–Laplace force due to an axisymmetric constant-volume distortion of wave number q. Inserting this growth rate into the MSC equations (4) yields the front velocity as a function of viscosity ratio, which was previously derived in Ref. 5. Figure 6 compares this prediction with our present numerical calculations.

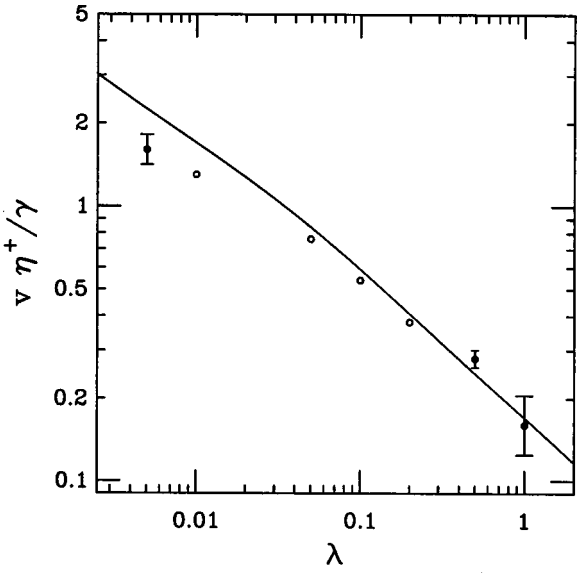

FIG. 6. Front velocity $v=v_{\mathrm{msc}}$ vs λ. The circles are the results of the numerical calculations, the line is the prediction of the MSC from Ref. 5.

Since the growth rate for the Rayleigh instability does not contain the physical process of retraction, we expect the MSC velocity to depart from the true front speed when the front and retraction speeds are comparable. This may be the source of disagreement between the MSC and the numerical simulations for $\lambda\geqslant 0.5$. As λ is increased beyond this value, retraction becomes more important until finally the simple picture of a propagating Rayleigh instability becomes invalid. As the lower values of viscosity ratio are approached, the boundary integral method eventually fails to conserve volume.[24] In Fig. 6 we only show data for runs in which the volume changed slightly (by no more than a few percent) if at all; nevertheless, since it is difficult assess the impact of these errors on the front velocity, we cannot say if this is the source of disagreement between the MSC and the numerical calculations for $\lambda<0.01$.[25]

While the front position advances smoothly in accord with the MSC picture, the behavior of the front shape encoded in the wave number q'_{num} and the inverse front width q''_{num} is more complicated. We find that these quantities are not constant but rather oscillate with approximately the period of pinching; however, they are always near the MSC values. Moreover, the fitted values for $q'_{\mathrm{num}}, q''_{\mathrm{num}}$ did not depend on the choice of fitting window, so it is the actual front shape that is oscillating. One example is shown in the bottom graph of Fig. 5. We conclude that the MSC captures

the gross features of the front shape but not the fine structure.

Given that we find the breakup process to be periodic in the viscosity range $\lambda = 0.005-0.1$, it is natural to ask if the MSC can predict the time t_{pinch} between primary pinching events, once the transients due to the initial shape settle down. A plausible but naive starting point is to use the shortest characteristic growth time, $t_{\text{pinch}} = \omega(q_{\max})^{-1}$, where $q_{\max}$ is the wave number of the fastest growing mode calculated from linear stability theory. However, it is well known that the fastest growing mode is not selected when the MSC is applicable. In the standard MSC treatment, there are in fact *two* selected wave numbers: q'_{msc}, the selected wave number in the *leading edge* of the front, and $q_0 = \text{Im}(\omega(q^*)+iq^* v_{\text{msc}})/v_{\text{msc}}$, the selected wave number in the *saturated* pattern.[8] Thus another candidate for the pinching time is $t_{\text{pinch}} = 2\pi/(q_0 v_{\text{msc}})$. However, as we pointed out in Ref. 5, we do not expect q_0 to be relevant to the Rayleigh problem since the saturated pattern has not continuously evolved from the leading edge of the front. Therefore we expect the appropriate wavelength to be $2\pi/q'_{\text{msc}}$. In Fig. 7 we show that the numerical simulations clearly favor the relation $t_{\text{pinch}} = 2\pi/(q'_{\text{msc}} v_{\text{msc}})$.

The behavior of the MSC quantities for small λ can be seen analytically by examining the growth rate in the limit of small wave number:[23,5]

$$\omega(q,\lambda) \sim \frac{\gamma}{2R_0\eta^+} \frac{(qR_0)^2[1-\lambda(2+4C)-4\lambda\ \log(qR_0/2)]}{8\lambda-(qR_0)^2(\lambda-1)[1+3\lambda(2+4C)+12\lambda\ \log(qR_0/2)]}, \tag{5}$$

where $C \approx 0.577$ is Euler's constant. Assuming $\lambda\ \log(qR_0) \ll 1$, (5) simplifies to

$$\omega(q,\lambda) \sim \frac{\gamma}{2R_0\eta^+} \frac{(qR_0)^2}{8\lambda+(qR_0)^2}. \tag{6}$$

Dominant balance of the MSC equations (4) implies $qR = O(\lambda^{1/2})$, $v_{\text{msc}} = O(\lambda^{-1/2})$; assuming these scalings with (4) and (6), we find

$$q'_{\text{msc}}R_0 \sim 2.26\lambda^{1/2},\quad q''_{\text{msc}}R_0 \sim 2.95\lambda^{1/2},\quad v_{\text{msc}}\eta^+/\gamma \sim 0.139\lambda^{-1/2} \tag{7}$$

(the scalings are found analytically, the prefactors were obtained by solving numerically the resulting transcendental equations). Note that our neglect of $\lambda\ \log(qR_0)$ is consistent with these scalings. For small enough λ, these quantities agree well with the results of numerically solving the MSC equations with the the full form of Tomotika's growth rate.

These results (7) are different from the scalings expected from the traditional linearized analysis. Using Tomotika's growth rate we have determined (numerically) as a function of λ the wave number $q_{\max}$ corresponding to the maximum growth rate, and have found $q_{\max} = O(\lambda^{1/4})$ for $\lambda \ll 1$. Indeed, this behavior can be seen analytically by retaining the axial curvature in (6) and approximating the growth rate by

$$\omega(q,\lambda) \sim \frac{\gamma}{2R_0\eta^+}(1-q^2R_0^2)\ \frac{(qR_0)^2}{8\lambda+(qR_0)^2}, \tag{8}$$

which has a fastest-growing mode scaling like $\lambda^{1/4}$. Moreover, to find the scaling of the fluid velocity, we can compute the flow profile in the linear approximation for $h \propto \exp(\omega t+iqz)$ in the small q (lubrication) limit. We find

$$w^-(r,z) = -\frac{2i}{qR_0}\left(1-\frac{r^2}{R_0^2}\right)\frac{h}{R_0}\frac{\gamma}{\eta^+}, \tag{9}$$

$$u^-(r,z) = \left(\frac{r^3}{R_0^3}-\frac{2r}{R_0}\right)\frac{h}{2R_0}\frac{\gamma}{\eta^+}, \tag{10}$$

where w is the axial velocity and u is the radial velocity. The flow velocity along the centerline $w^-(r=0,z)$ scales as $1/q$ for small q, so for $q = q_{\max}$, $w^- = O(\lambda^{-1/4})$. Note that the scalings of the MSC velocity and wave number obey the same relation, $v_{\text{msc}}q'_{\text{msc}} = O(1)$. Unfortunately, we were not able to extend the simulations to small enough λ to verify these asymptotic relations.

Finally, we remark about the implications of the divergence in velocity and wavelength as $\lambda \to 0$. It is certainly true that finite-size effects can cut off the growing velocity when the drop size is comparable to the scale of the fluid flow. It is also true that the zero-Reynolds-number approximation will break down for sufficiently small λ. In particular, imagine decreasing the inner viscosity while holding the properties of the outer fluid fixed. To estimate when inertia becomes im-

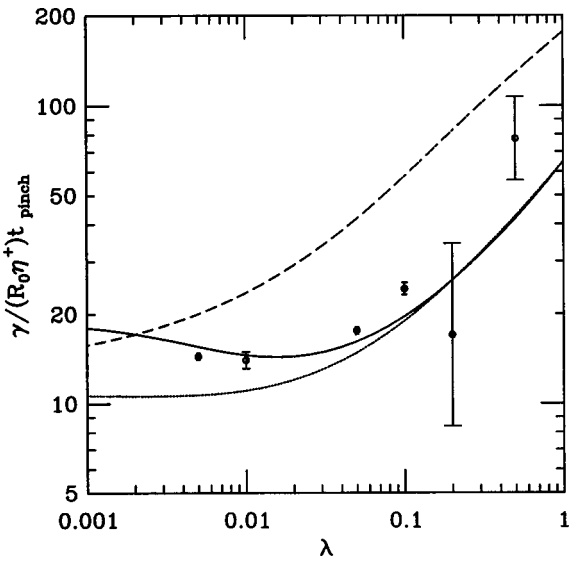

FIG. 7. Various predictions for the primary pinch time. Solid line is $2\pi/(q'_{\text{msc}}v_{\text{msc}})$, dotted line is $2\pi/(q_0 v_{\text{msc}})$, and the dashed line is $1/\omega(q_{\max})$. The circles are from the simulation. The breakup is aperiodic for $\lambda \geqslant 0.2$, leading to a distribution of droplet sizes.

portant, consider the *inner* Reynolds number $Re=\rho|\mathbf{u}\cdot\nabla\mathbf{u}|/(\eta^-|\nabla^2\mathbf{u}|)$, where ρ is the density of the (neutrally buoyant) inner fluid. Using (10) and taking $h\approx R_0$, we find $|\mathbf{u}\cdot\nabla\mathbf{u}|\approx qw$, and $|\nabla^2\mathbf{u}|\approx w/R_0^2$, or $Re\approx\rho R_0\gamma/(\eta^+\eta^-)=\rho R_0\gamma/(\eta^{+2}\lambda)$. Thus, when λ is greater than approximately $\gamma R_0\rho/(\eta^{+2})$, the inner Reynolds number will be approximately unity and the Stokes equations will be invalid.

IV. CONCLUDING REMARKS

In conclusion, we have shown that the breakup of elongated drops can proceed via front propagation for the viscosity ratios in the range $\lambda=0.005-1.0$. Remarkably, despite the complex nature of the discontinuous dynamics, the marginal stability criterion gives a good description of the gross quantitative features of the shape evolution, such as the front velocity and shape, and the pinch-off time. There are many experimental systems which could be used to test our results. The most natural candidate is the four-roll mill, in which a planar hyperbolic flow stretches a spherical drop into a long thread.[9] When this flow ceases, the relaxation or breakup of the thread can be studied. Other possibilities are capillary bridges stabilized by electric or magnetic fields[26] or very viscous jets. Experimental confirmation of our picture of propagating topological transitions would be an important contribution to the understanding of interface motion in fluid dynamics.

ACKNOWLEDGMENTS

T.R.P. thanks Dartmouth College for hospitality. This work was supported by NSF Presidential Faculty Fellowship Grant no. DMR 93-50227 (REG), and the Petroleum Research Fund (Grant No. 28690-AC9) (DFZ and HAS).

[1] R. Bar-Ziv and E. Moses, ''Instability and 'pearling' states produced in tubular membranes by competition of curvature and tension,'' Phys. Rev. Lett. **73**, 1392 (1994); R. Bar-Ziv, T. Tlusty, and E. Moses, ''Critical dynamics in the pearling instability of membranes,'' Phys. Rev. Lett. **79**, 1158 (1997).

[2] P. Nelson, T. Powers, and U. Seifert, ''Dynamic theory of pearling instability in cylindrical vesicles,'' Phys. Rev. Lett. **74**, 3384 (1995); R. Granek and Z. Olami, ''Dynamics of Rayleigh-like instability induced by laser tweezers in tubular vesicles of self-assembled membranes,'' J. Phys. II France **5**, 1348 (1995); R. E. Goldstein, P. Nelson, T. R. Powers, and U. Seifert, ''Front propagation in the pearling instability of tubular vesicles'' J. Phys. II France **6**, 767 (1996).

[3] J. Plateau, *Statique experimentale et theorique des liquides soumis aux seules forces moleculaires* (Gautier-Villars, Paris, 1873); Lord Rayleigh, ''On the instability of jets,'' Proc. London Math. Soc. **10**, 4 (1879); Lord Rayleigh, ''On the instability of a cylinder of viscous liquid under capillary force,'' Philos. Mag. **34**, 145 (1892).

[4] S. Chandrasekhar, *Hydrodynamic and Hydromagnetic Stability* (Oxford University Press, Oxford, 1961).

[5] T. R. Powers and R. E. Goldstein, ''Pearling and pinching: propagation of Rayleigh instabilities,'' Phys. Rev. Lett. **78**, 2555 (1997).

[6] M. C. Cross and P. C. Hohenberg, ''Pattern formation outside of equilibrium,'' Rev. Mod. Phys. **65**, 851 (1993).

[7] S. J. Di Bartolo and A. T. Dorsey, ''Velocity selection for propagating fronts in superconductors,'' Phys. Rev. Lett. **77**, 4442 (1996).

[8] G. Dee and J. S. Langer, ''Propagating pattern selection,'' Phys. Rev. Lett. **50**, 383 (1983); E. Ben-Jacob, H. Brand, G. Dee, L. Kramer, and J. S. Langer, ''Pattern propagation in nonlinear dissipative systems,'' Physica (Utrecht) **14D**, 348 (1985); W. van Saarloos, ''Front propagation into unstable states,'' Phys. Rev. A **37**, 211 (1988); W. van Saarloos, ''Front propagation into unstable states, II,'' Phys. Rev. A **39**, 6367 (1989).

[9] H. A. Stone, B. J. Bentley, and L. G. Leal, ''An experimental study of transient effects in the breakup of viscous drops,'' J. Fluid Mech. **173**, 131 (1986). See also the seminal work of G. I. Taylor, ''The formation of emulsions in definable fields of flow,'' Proc. R. Soc. London, Ser. A **146**, 501 (1934).

[10] This result is reminiscent of the fact that the appearance of the von Kármán vortex street in the wake of a cylinder is related to the transition of the wake instability from absolute to convective. This transition can be understood using linear analysis; e.g. G. S. Triantafyllou, K. Kupfer, and A. Bers, ''Absolute instabilities and self-sustained oscillations in the wakes of circular cylinders,'' Phys. Rev. Lett. **59**, 1914 (1987) and references therein.

[11] C. Pozrikidis, *Boundary Integral and Singularity Methods for Linearized Viscous Flow* (Cambridge University Press, Cambridge, 1992). See also A. Z. Zinchenko, M. A. Rother, and R. H. Davis, ''A novel boundary-integral algorithm for viscous interactions of deformable drops,'' Phys. Fluids **9**, 1493 (1997).

[12] The kernels in (3) are

$$J_{ij}(\mathbf{x},\mathbf{y})=\frac{\delta_{ij}}{|\mathbf{x}-\mathbf{y}|}+\frac{(\mathbf{x}-\mathbf{y})_i(\mathbf{x}-\mathbf{y})_j}{|\mathbf{x}-\mathbf{y}|^3},$$

$$K_{ijk}(\mathbf{x},\mathbf{y})=-6\frac{(\mathbf{x}-\mathbf{y})_i(\mathbf{x}-\mathbf{y})_j(\mathbf{x}-\mathbf{y})_k}{|\mathbf{x}-\mathbf{y}|^5}.$$

[13] J. Tanzosh, M. Manga, and H. A. Stone, ''Boundary integral methods for viscous free-boundary problems: Deformation of single and multiple fluid-fluid interfaces,'' in *Proceedings of Boundary Element Technologies VII*, edited by C. A. Brebbia and M. S. Ingber (Computational Mechanics, Boston, 1992), p. 19.

[14] J. Eggers and T. F. DuPont, ''Drop formation in a one-dimensional approximation of the Navier-Stokes equation,'' J. Fluid Mech. **262**, 205 (1994); D. T. Papageorgiou, ''Analytical description of the breakup of liquid jets,'' J. Fluid Mech. **301**, 109 (1995).

[15] H. A. Stone and L. G. Leal, ''Relaxation and breakup of an initially extended drop in an otherwise quiescent fluid,'' J. Fluid Mech. **198**, 399 (1989).

[16] H. Lamb, *Hydrodynamics*, 6th ed. (Cambridge University Press, Cambridge, 1993).

[17] The front parameters were determined through a nonlinear least-squares fitting algorithm [W. H. Press, B. P. Flannery, S. A. Teukolsky, and W. T. Vetterling, *Numerical Recipes in C* (Cambridge University Press, New York, 1988)].

[18] Many of the breakup events involved smaller, satellite droplets, the analysis of which we have not pursued.

[19] Figure 3c of M. Tjahjadi, H. A. Stone, and J. M. Ottino, ''Estimating interfacial tension via relaxation of drop shapes and filament breakup,'' AIChE. J. **40**, 385 (1994).

[20] R. J. Briggs, *Electron Stream Interactions with Plasmas* (MIT Press, Cambridge, MA, 1964); E. M. Lifshitz and L. P. Pitaevskii, *Physical Kinetics* (Butterworth-Heinemann Ltd., Oxford, 1981), Sec. 62-63.

[21] R. Fisher, ''The advance of advantageous genes,'' Ann. Eugenics **7**, 355 (1937); A. Kolmogorov, I. Petrovsky, and N. Piskunov, ''Étude de l'equation de la diffusion avec croissance de la quantité de matiére et son application à un probleme biologique,'' Bull. Univ. Moskou, Ser. Internat., Sec. A **1**, 1 (1937).

[22] D. G. Aronson and H. F. Weinberger, in *Partial Differential Equations and Related Topics*, edited by J. A. Goldstein (Springer-Verlag, Heidelberg, 1975), 5.

[23] S. Tomotika, ''On the instability of a cylindrical thread of a viscous liquid surrounded by another viscous fluid,'' Proc. R. Soc. London, Ser. A **150**, 322 (1935).

[24] It is well known that numerical boundary integral methods become less accurate at small λ (Ref. 11). We found that for $\lambda=0.001$ the volume of the drop changed by about 10% during the continuous evolution.

[25] There is another possible source of error. In the MSC picture, the front accelerates to the MSC velocity with a relaxation time that scales as $(q''_{\mathrm{msc}})^{-1}$ (Refs. 8, 20). Thus, when retraction is unimportant, we would expect our numerical results to lie below the MSC curve. This discrepancy should be greatest for the smallest values of λ we considered, since it is precisely those values for which q''_{msc} is getting small (Ref. 5). However, we saw no evidence of acceleration of the front in the numerical calculations.

[26] S. Sankaran and D. A. Saville, ''Experiments on the stability of a liquid bridge in an axial electric field,'' Phys. Fluids A **5**, 1081 (1993).